tRNA tK^{UUU}, tQ^{UUG}, and tE^{UUC} wobble position modifications fine-tune protein translation by promoting ribosome A-site binding

Vanessa Anissa Nathalie Rezgui[a,1], Kshitiz Tyagi[b,1], Namit Ranjan[a,1], Andrey L. Konevega[c,d], Joerg Mittelstaet[c], Marina V. Rodnina[c], Matthias Peter[a], and Patrick G. A. Pedrioli[b,2]

[a]Department of Biology, Institute of Biochemistry, Eidgenössiche Technische Hochschule Zürich, 8093 Zürich, Switzerland; [b]Scottish Institute for Cell Signalling, College of Life Sciences, University of Dundee, DD1 5EH Dundee, United Kingdom; [c]Department of Physical Biochemistry, Max Planck Institute for Biophysical Chemistry, 37077 Göttingen, Germany; and [d]Molecular and Radiation Biophysics Department, B. P. Konstantinov Petersburg Nuclear Physics Institute, 188300 Gatchina, Russia

Edited by Dieter Söll, Yale University, New Haven, CT, and approved June 12, 2013 (received for review January 15, 2013)

tRNA modifications are crucial to ensure translation efficiency and fidelity. In eukaryotes, the *URM1* and *ELP* pathways increase cellular resistance to various stress conditions, such as nutrient starvation and oxidative agents, by promoting thiolation and methoxycarbonylmethylation, respectively, of the wobble uridine of cytoplasmic $tRNA^{UUU}_{Lys}$ (tK^{UUU}), $tRNA^{UUG}_{Gln}$ (tQ^{UUG}), and $tRNA^{UUC}_{Glu}$ (tE^{UUC}). Although in vitro experiments have implicated these tRNA modifications in modulating wobbling capacity and translation efficiency, their exact in vivo biological roles remain largely unexplored. Using a combination of quantitative proteomics and codon-specific translation reporters, we find that translation of a specific gene subset enriched for AAA, CAA, and GAA codons is impaired in the absence of *URM1*- and *ELP*-dependent tRNA modifications. Moreover, in vitro experiments using native tRNAs demonstrate that both modifications enhance binding of tK^{UUU} to the ribosomal A-site. Taken together, our data suggest that tRNA thiolation and methoxycarbonylmethylation regulate translation of genes with specific codon content.

translation regulation | SILAC | systems biology

To date, over 100 modifications of the four canonical RNA nucleotides have been described (1, 2). However, their biological relevance remains poorly understood. In yeast, over 25 distinct nucleotide modifications have been identified in tRNA molecules. Modifications at or near the anticodon are thought to be functionally important for translational efficiency and fidelity (3). In particular, the wobble position, residue 34, has emerged as a hot spot for modifications that restrict or increase wobbling (4, 5).

Uridine-34 (U_{34}) is universally modified to 5-methyl-2-thio derivatives in the tRNAs encoding for lysine, glutamine, and glutamic acid, namely tK^{UUU}, tQ^{UUG}, and tE^{UUC}, respectively (6). Specifically, in yeast and higher eukaryotes, these tRNAs contain a 5-methoxycarbonylmethyl-2-thiouridine ($mcm^5s^2U_{34}$). These modified tRNAs belong to split codon box families in which the synonymous A- and G-ending codons code for a different amino acid than U- and C-ending ones. In vitro, tRNAs containing either the s^2 or the mcm^5 modification on U_{34} are able to bind and translocate in ribosomes primed with A- and G-ending codons, but not U- and C-ending ones (7, 8). However, accurate protein translation in vivo also relies on correct charging by the aminoacyl-tRNA synthetases (9), tRNA gene copy numbers, and tRNA posttranscriptional modifications (10). Therefore, approaches to measure the in vivo relevance of RNA modifications and compare it to in vitro results are necessary to integrate these multifactorial contributions.

In yeast, the $mcm^5s^2U_{34}$ modification relies on the *URM1* pathway for the s^2 (11–15) and on the *ELP* pathway for the mcm^5 addition (16). The *URM1* pathway contains the ubiquitin related modifier 1 (Urm1), its activating enzyme (Uba4), as well as the two proteins Needs Cla4 to Survive 2 and 6 (Ncs2 and Ncs6, respectively), and ThioUridine Modification protein 1 (Tum1), (12). The *ELP* pathway includes the six subunits of the Elp-complex (Elp1–6) and the TRna Methyltransferase complex containing Trm9 and Trm112 (16). Although thiolation is found exclusively on tK^{UUU}, tQ^{UUG}, and tE^{UUC}, Elp-dependent modifications are found on eight additional tRNAs.

Yeast cells lacking a functional *URM1* or *ELP* pathway are sensitive to a wide range of drugs, suggesting a regulatory role of these modifications in translation under stress conditions. Moreover, U_{34} hypomodification of cytoplasmic tRNAs has been linked with defects in neural function and development in *Caenorhabditis elegans* (17, 18), with familial dysautonomia (19), and nonthiolated mitochondrial tRNAs are associated with the human disease myoclonic epilepsy with ragged red fibers (20). However, the underlying cellular and molecular mechanisms affected by lack of thiolation and methoxycarbonylmethylation are poorly understood.

Here, we present a proteome-wide analysis of changes in protein abundance induced in cells lacking tRNA thiolation and methoxycarbonylmethylation. We show that in vivo these tRNA modifications are not required for general translation, but specifically modulate translation of mainly AAA-, CAA-, and GAA-rich genes. Importantly, biochemical analysis using purified components revealed that these modifications of U_{34} specifically increase ribosomal A-site binding and peptide bond formation in vitro.

Results

Lack of *URM1* Affects Only a Small Subset of the Proteome. Relative protein abundance in *urm1*Δ yeast cells was compared with wild-type cells by stable isotope-labeling by amino acids in cell culture (SILAC) -based quantitative mass spectrometry. The density distribution of protein abundance ratios from a single biological replicate shows that most of the proteome is unaffected by lack of thiolation and that only a small fraction of proteins are differentially expressed (Fig. 1*A*). Similarly, quantification of [^{35}S] Met and [^{35}S]Cys incorporation into newly synthesized proteins

Author contributions: V.A.N.R., K.T., N.R., A.L.K., M.V.R., M.P., and P.G.A.P. designed research; V.A.N.R., K.T., N.R., A.L.K., J.M., and P.G.A.P. performed research; V.A.N.R., K.T., N.R., A.L.K., J.M., M.V.R., M.P., and P.G.A.P. contributed new reagents/analytic tools; V.A.N.R., K.T., N.R., A.L.K., J.M., and P.G.A.P. analyzed data; and V.A.N.R., K.T., N.R., A.L.K., M.P., and P.G.A.P. wrote the paper.

The authors declare no conflict of interest.

This article is a PNAS Direct Submission.

Freely available online through the PNAS open access option.

[1]V.A.N.R., K.T., and N.R. contributed equally to this work.

[2]To whom correspondence should be addressed. E-mail: p.g.a.pedrioli@dundee.ac.uk.

This article contains supporting information online at www.pnas.org/lookup/suppl/doi:10.1073/pnas.1300781110/-/DCSupplemental.

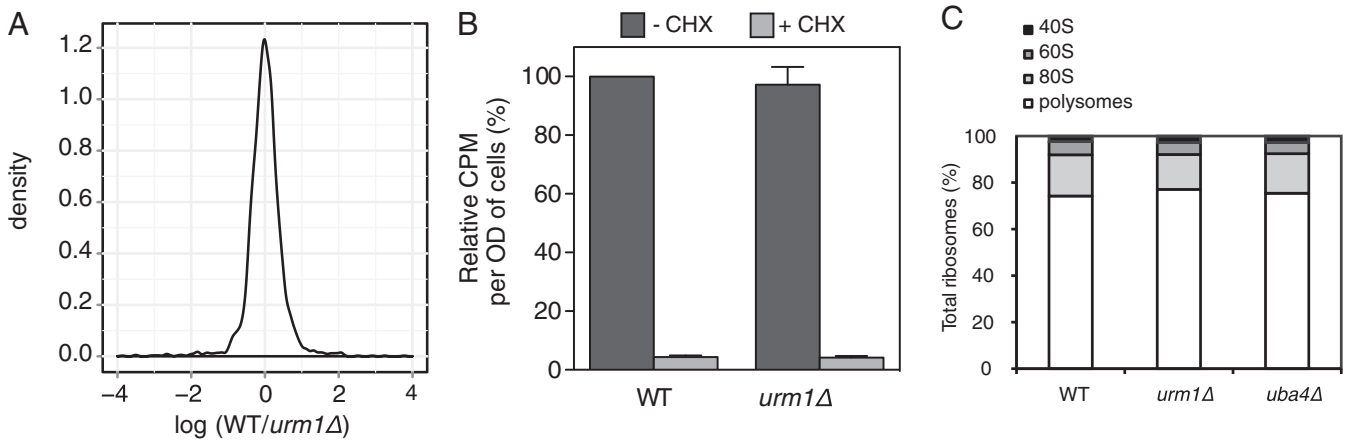

Fig. 1. General translation is unaffected by lack of *URM1*. (*A*) Density plot of $\log_2$(WT/*urm1*Δ) protein abundance ratios from a single SILAC-based proteomics experiment. (*B*) Wild-type and *urm1*Δ cells were pulsed with [^{35}S]Met and [^{35}S]Cys in the presence (+) or absence (–) of cycloheximide (CHX). [^{35}S] incorporation into proteins was quantified by liquid scintillation counting. Counts per minute were normalized to the wild-type value. Data show mean ± SEM of three independent experiments. (*C*) Quantification of the polysome profiles from wild-type, *urm1*Δ, and *uba4*Δ cells separated on a 6–45% sucrose gradient showing the distribution of 40S, 60S, and 80S particles and polysomes as percentage of total ribosomes from the average of three independent experiments. See also Fig. S1.

by pulse-chase labeling showed no significant difference between wild-type and *urm1*Δ cells (Fig. 1*B*). Likewise, polysome profile analysis revealed that the percentage of polysomes and the ratio of 40S, 60S, and 80S particles in *urm1*Δ and *uba4*Δ cells were comparable to wild-type controls (Fig. 1*C* and Fig. S1*A*). Taken together, these experiments suggest that thiolation of U_{34} does not differentially impair general protein translation under standard growth conditions.

Lack of *URM1* or *ELP3* Impairs Protein Expression of AAA-, CAA-, AAG-, and GAA-rich mRNAs. To identify differentially expressed proteins in the absence of a functional *URM1* pathway, we designed a SILAC-based experimental workflow aimed at maximizing proteome coverage and sensitivity (Fig. 2*A* and Fig. S1*B*). Statistical significance of protein ratios from six biological replicates was calculated using an empirical Bayes moderated *t* test (21). To maximize proteome coverage, the samples were extensively fractionated at the protein and peptide levels and analyzed using a combination of multiple database search engines (22). Overall, we identified 3,818 proteins, corresponding to 57% of the predicted yeast proteome, at a 1% false-discovery rate (FDR) at the protein level. Small variations in the distribution of protein ratios across the biological replicates were normalized using median normalization (Fig. S1*C*). The data did not show any trend in protein ratios vs. number of peptides used for the computation either before or after normalization (Fig. S1*D*). Statistical analysis identified 267 proteins to be significantly (5% FDR) down-regulated and 286 proteins to be up-regulated in *urm1*Δ cells (Fig. 2*B* and Dataset S1, Table S1). Gene ontology analysis of the differentially expressed proteins showed that down-regulated proteins were enriched for anabolic processes, such as translation initiation and elongation, whereas up-regulated proteins were enriched for catabolic processes such as proteasomal degradation (Dataset S1, Tables S2 and S3). To assess whether the mcm^5 modification similarly affects protein abundance in *elp3Δ* mutants, we used a second SILAC-based proteomics approach that compared protein abundances between *urm1Δ* and *elp3Δ* cells. This analysis quantified 243 (85%) from the significantly up-regulated and 199 (74.5%) from the significantly down-regulated proteins identified in the *urm1Δ* vs. wild-type experiment (Dataset S1, Table S4). Importantly, the levels of all these proteins were comparable in *urm1*Δ and *elp3*Δ cells, implying that the *URM1*- and *ELP*-pathways control an overlapping set of target proteins. In total, only 12 proteins, two of which were Elp3 and His3 (the histidine auxotrophic marker used to delete *ELP3*), were found to be significantly changing in *elp3Δ* compared with the *urm1Δ* mutants.

To identify the codons that best separated the significantly up- and down-regulated datasets, we performed an unsupervised machine learning analysis using a random forest algorithm of the *urm1Δ* vs. wild-type data. A plot of variable importance (Fig. 2*C*) illustrates that the codons AAA, CAA, AAG, GGG, and GAA, in decreasing order of their importance, were the best at classifying the data in up- or down-regulated sets. Further analysis suggested that codons AAA, CAA, and GAA, and to a lesser extent AAG, were significantly enriched in the down-regulated dataset, whereas GGG was enriched in the up-regulated dataset and was associated with up-regulated mRNAs (Fig. 2*D*, Figs. S2 and S3, and Dataset S1, Tables S5 and S6). The results of the analysis were first tested for stability in silico by varying the random seed. We then tested the predictions in vivo by assessing the ability of individual tRNAs to rescue the differential protein abundance using SILAC-based proteomics of wild-type vs. *urm1*Δ cells overexpressing tK^{UUU}, tQ^{UUG}, and tE^{UUC}, either individually or in combination. The heatmap in Fig. 2*E* shows that overexpression of all three tRNA species reverts most of the differentially expressed proteins back to wild-type levels. This finding indicates that *URM1* activity in tRNA thiolation is mainly responsible for the observed differential protein abundance. Complete clustering using Euclidean distances recapitulates and validates the relative importance of different codons predicted by the random forest (dendrogram in Fig. 2*E*).

Down-regulated candidates exhibiting a significant codon-bias were selected for further analysis (Fig. 3 *A* and *B*). Protein abundance was measured by Western blotting and confirmed reduced expression levels in *urm1*Δ cells (Fig. 3*C* and Fig. S4*A*). Quantitative real-time PCR revealed that mRNA abundance of all but one candidate were comparable in wild-type and *urm1*Δ cells (Fig. 3*D* and Fig. S4*B*), implying that changes at the protein level are responsible for their differential protein expression. To discriminate between differential degradation and translation, we quantified the stability of Cms1 and Ypl199c in wild-type and *urm1*Δ cells after blocking translation by cycloheximide (Fig. 3 *E* and *F* and Fig. S4*C*). Both proteins were degraded with half-lives of ~60 and 70 min, respectively, in wild-type and *urm1*Δ cells, implying that the observed changes in protein levels are caused by reduced translation rates in *urm1*Δ cells. Taken together,

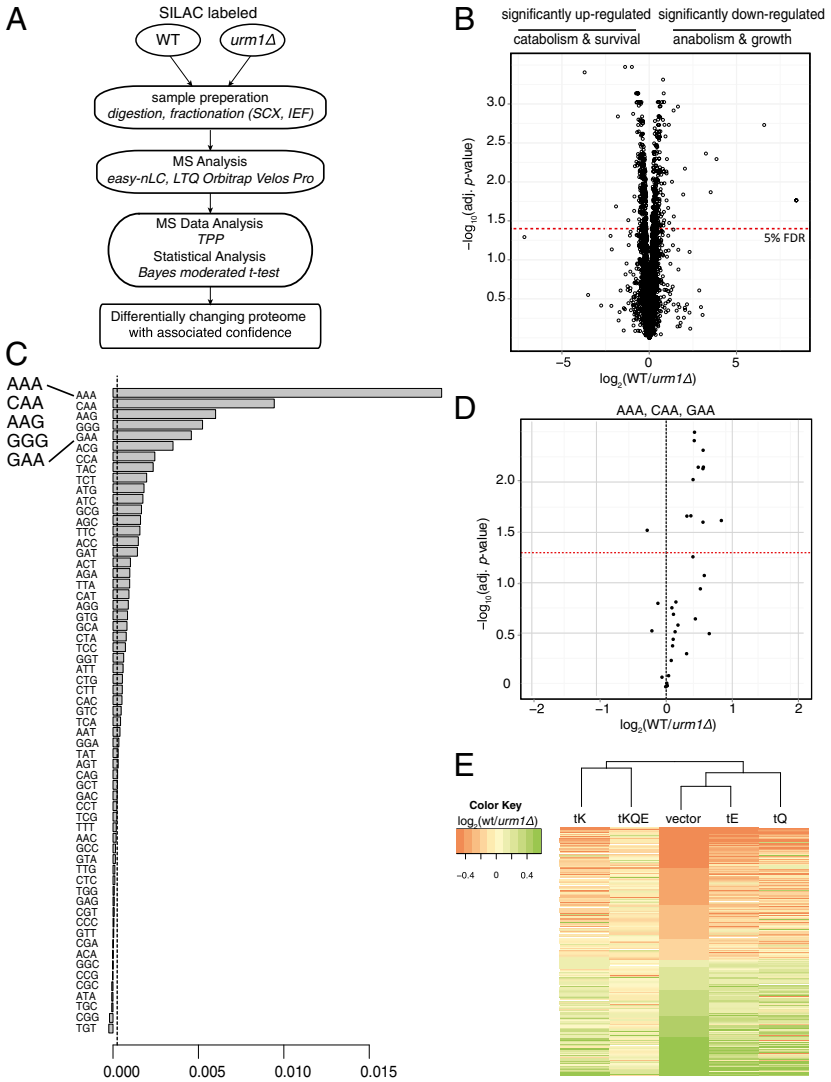

Fig. 2. *URM1* is important for efficient expression of a subset of AAA-, CAA-, AAG-, and GAA-rich genes. (*A*) Schematic representation of the quantitative proteomics workflow used to assess differential translation in *urm1*Δ cells. (*B*) Volcano plot of protein abundance ratios vs. their bayes normalized *t* test calculated confidence. Results shown are of six biological replicates. Red dotted line: 5% FDR chosen as statistical significance. (*C*) Barplot representation of the variable importance learned by a random forest algorithm used to predict the ability of different codon abundances in classifying proteins in significantly up- and down-regulated sets. Dotted line: absolute value of the lowest predictor. (*D*) Proteins with the corresponding highest frequency (1% of the genome) of AAA, CAA, and GAA codons represented in the volcano plot from Fig. 2*B*. Red dotted line: 5% FDR. (*E*) Heatmap of $\log_2$(WT/*urm1*Δ) protein abundance ratios of the significantly up- and down-regulated proteins from Fig. 2*B* in cells overexpressing tK^{UUU}, tQ^{UUG}, and tE^{UUC} individually or in combination compared with cells without plasmid. Columns are clustered based on Euclidean distance. Figs. S1–S3.

these data suggest that efficient translation of mRNA molecules rich in AAA, CAA, GAA, and AAG codons requires functional *URM1* and *ELP* pathways in vivo.

s^2 and mcm^5 Modifications of U_{34} in tK^{UUU}, tQ^{UUG}, and tE^{UUC} Are Required for Codon-Specific Translation in Vivo. To further assess codon use and translation regulation, we constructed an in vivo codon-specific translation reporter (Fig. 4*A*) consisting of quadruple-cyan fluorescent protein (CFP) (4× CFP) and quadruple-venus (4× YFP, yellow fluorescent protein), both inducible by the addition of β-estradiol (23). CFP and YFP are very similar and stable molecules, thus ruling out codon composition and degradation effects. Additionally, YFP and CFP can be readily quantified in vivo by fluorescence microscopy in single cells (Fig. S5*A*), thereby accounting for cell-to-cell variations and extrinsic effects, such as cell-cycle stage (24). Although YFP fluorescence reports on codon-specific translation caused by a "codon trap" of N-terminally inserted codon-enriched sequences, CFP expression controls for the general expression capacity of the same cell (Fig. S5*B*).

We first analyzed a codon-trap of 10 consecutive CAA codons, $(CAA)_{10}$, in a time-course experiment. After a delay of 45 min, corresponding to the maturation time of the fluorophores, both wild-type and *urm1*Δ cells showed reporter expression, but the expression in *urm1*Δ cells was significantly slower and only reached ∼60% of wild-type expression after 5 h (Fig. 4 *B* and *C*). Reexpression of Urm1 from a centromeric plasmid restored efficient translation (Fig. S5*C*). A similar defect was also observed in *uba4*Δ and *elp3*Δ cells (Fig. 4*C*), implying that s^2 and the mcm^5 modifications are both required for efficient translation. Similarly, tRNA thiolation also influenced translation of $(AAA)_{10}$ or $(GAA)_{10}$ codon-traps (Fig. 4*D*). Interestingly, inclusion of the synonymous G-ending codon, $(AAG)_{10}$, recognized by the non-thiolated tK^{UUC}, did not affect translation of YFP in *urm1*Δ cells, demonstrating that the *URM1*-dependent decrease in reporter expression is specific to the codon use and not the amino acid composition. Taken together, these data suggest that efficient translation of AAA-, CAA-, and GAA-rich reporters requires functional *URM1* and *ELP* pathways in vivo.

U_{34} Modifications Enhance Ribosomal A-Site Binding and Dipeptide Formation Rates in Vitro. To investigate how thiolation and methoxycarbonylmethylation promote efficient translation of cognate codons, we compared the effects of native and hypomodified yeast tRNAs on binding to the A-site of the ribosome and dipeptide formation in vitro (Fig. 5*A*). $tRNA^{Lys}$ isolated from wild-type, *urm1*Δ, or *elp3*Δ yeast cells were aminoacylated (aa) with [^{14}C]-labeled lysine and incubated with EF-Tu·GTP to form ternary complex. The [^{14}C]Lys-$tRNA^{Lys}$ ternary complex was mixed with 70S initiation complex from *Escherichia coli* loaded with f[^{3}H]Met-$tRNA^{fMet}$ and mRNA containing an AAA

BIOCHEMISTRY

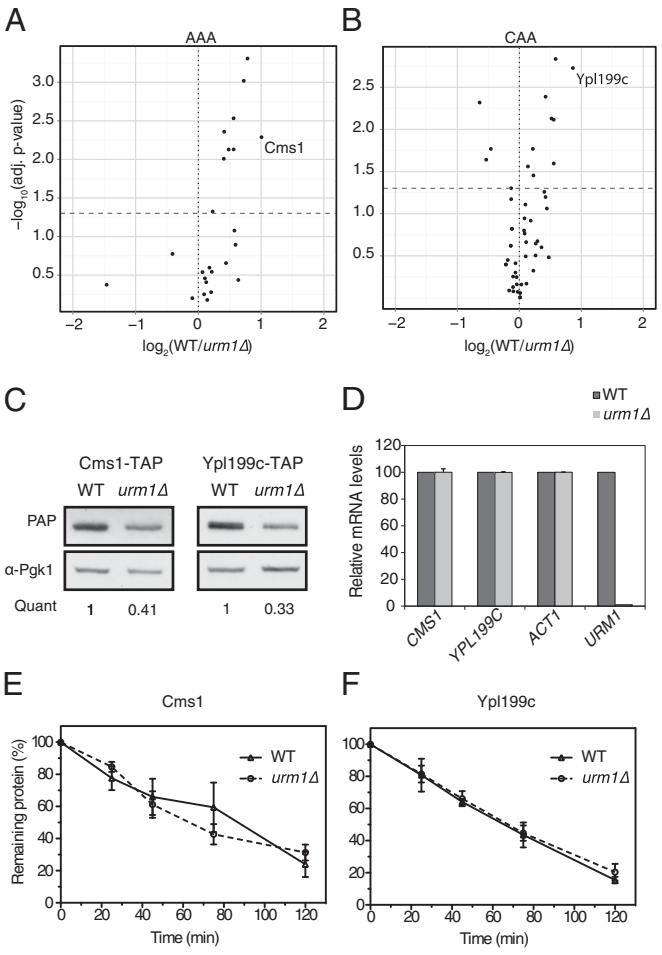

Fig. 3. The *URM1*-pathway specifically regulates translation of Cms1 and Ypl199c. (*A* and *B*) Volcano plots of protein abundance ratios with statistical significance measured by quantitative proteomics of the top 1.5% yeast genes with the highest (*A*) AAA or (*B*) CAA codon frequency. (*C*) Western blot of TAP-tagged Cms1 or Ypl199c from wild-type and *urm1*Δ cells using PAP antibodies or anti-Pgk1 as loading control. The quantification indicates the *urm1*Δ/WT protein abundance ratio averaged from three independent experiments. (*D*) The mRNA levels of *CMS1* and *YPL199C* and the *ACT1* or *URM1* controls were measured by quantitative PCR in wild-type and *urm1*Δ cells. Data show the mean ± SEM of three independent experiments. (*E* and *F*) The protein stability of TAP-tagged (*E*) Cms1 and (*F*) Ypl199c in wild-type and *urm1*Δ cells was determined by Western blot of extracts prepared at the indicated time points (min) after CHX addition. Protein amount over time were compared with amount at time 0. Data show the mean ± SEM of three independent experiments. See also Figs. S2 and S4.

codon following the AUG initiation codon, and subsequently the A-site binding was measured. Interestingly, A-site binding of aa-tRNA^{Lys} from *urm1Δ* was decreased by 60% compared with wild-type controls (Fig. 5*B*), demonstrating an important role of tRNA thiolation to enhance cognate codon binding. A similar effect was observed with tRNAs extracted from *elp3*Δ cells that lack the mcm^5 modification (Fig. 5*B*), suggesting that both modifications enhance A-site binding. As a control, [^{14}C]Phe-tRNA^{Phe} ternary complex was mixed with 70S initiation complex from *E. coli* loaded with f[^{3}H]Met-tRNA^{fMet} and mRNA containing an UUC codon following the AUG initiation codon. As expected, the A-site binding of [^{14}C]Phe-tRNA^{Phe} from wild-type, *urm1*Δ, or *elp3*Δ cells was not significantly different (Fig. 5*C*), demonstrating that the observed binding defects of [^{14}C]Lys-tRNA^{Lys} are indeed caused by the missing U_{34} modifications.

To determine the kinetic parameters of A-site binding, ribosomal pretranslocation complexes bearing fMet[^{14}C]Lys-tRNA^{Lys} were prepared and peptidyl-tRNA dissociation was followed by nitrocellulose binding assay. The equilibrium dissociation constant, K_d, and the rate constant of tRNA dissociation (k_{off}) from and association (k_{on}) with the A-site were calculated from the apparent dissociation rates and the final level of the reaction. Strikingly, the k_{on} for peptidyl-tRNA^{Lys} from *urm1Δ* cells (5×10^{-3} $s^{-1}\cdot\mu M^{-1}$) and *elp3*Δ cells (5.6×10^{-3} $s^{-1}\cdot\mu M^{-1}$), were about three-times lower than for tRNAs from wild-type control cells (1.5×10^{-2} $s^{-1}\cdot\mu M^{-1}$), whereas k_{off} was higher with tRNA^{Lys} from *urm1*Δ cells (1.3×10^{-3} s^{-1}) and *elp3*Δ cells (1×10^{-3} s^{-1}) compared with tRNA^{Lys} from wild-type controls (6.6×10^{-4} s^{-1}) (Fig. 5*D*).

Because the final step in decoding results in peptide bond formation, we measured k_{pep}, the rate of ribosome-catalyzed formation of f[^{3}H]Met[^{14}C]Lys-tRNA^{Lys} dipeptides, using quench-flow analysis with rapid mixing of an excess of initiation complex with ternary complex (EF-Tu·GTP·[^{14}C]Lys-tRNA^{Lys}). Dipeptide formation was five-times slower with aa-tRNA^{Lys} tRNA from *urm1*Δ cells compared with wild-type with apparent rate constants, k_{pep}, of 0.2 s^{-1} and 1 s^{-1}, respectively (Fig. 5*E*). Together, these in vitro experiments demonstrate that wobble position modifications stabilize cognate codon-anticodon interactions at the ribosome, and thereby enhances the efficiency of translation.

Discussion

U_{34} Modifications Stabilize Binding of Cognate tRNAs to the A-Site and Promote Peptide Bond Formation. Our in vitro and in vivo experiments show that the s^2 and the mcm^5 modifications at the wobble position stabilize binding of cognate tRNAs, raising the possibility that tRNA modifications at the anticodon loop may generally enhance efficiency and fidelity of translation. Consistent with this notion, Trm9, involved in the mcm^5 modification, was recently shown to contribute to translation fidelity upon stress conditions (25). In *Saccharomyces cerevisae*, loss of thiolation does not abolish the presence of the mcm^5 modification, and cells lacking either mcm^5 or s^2 are viable. However, simultaneous loss of mcm^5 and s^2 is lethal (26), suggesting that these U_{34} modifications cooperatively promote translation. Indeed, previous in vitro studies showed that a synthesized anticodon stem loop fragment of human LYS3 tRNA hASL$_{Lys}^{UUU}$ lacking the mcm^{5}s^{2}U$_{34}$ and t^{6}A$_{37}$ modifications was unable to bind to AAA and AAG codons at the ribosomal A-site (27, 28). In this study, we used native tRNAs isolated from mutant yeast cells to examine the effect of the loss of a single tRNA modification on ribosomal binding. These data suggest that *URM1*- and *ELP*-mediated U_{34} modifications cooperate to increase binding of cognate tRNAs to the ribosomal A-site and subsequent peptide bond formation, thereby promoting efficient protein translation.

U_{34} Thiolation and Methoxycarbonylmethylation Control Efficient Translation of Specific mRNAs in Vivo. To better understand the in vivo biological relevance of tRNA wobble uridine thiolation, we used an unbiased data-driven approach to analyze the differential proteome of *urm1*Δ and wild-type cells. Bioinformatic analysis revealed that thiolation is required for the efficient expression of mRNAs rich in the cognate AAA, CAA, and GAA codons. Previous in vitro studies implicated thiolation in the efficient recognition of G-ending codons (7, 29). Interestingly, we also found differential translation of mRNAs rich in AAG but not CAG or GAG codons in *urm1*Δ cells. In vivo, G-ending codons are recognized by cognate, nonthiolated tRNAs. Yeast cells lacking tQ^{CUG} or tE^{CUC} are nonviable, suggesting that the thiolated tQ^{UUG} and tE^{UUC} cannot efficiently recognize CAG and GAG codons (30). However, AAG codons are preferentially used in highly expressed proteins, and tK^{UUU} might be required to supplement the translational capacity for these AAG-rich proteins. Remarkably, the synthetic translation reporters did not detect a

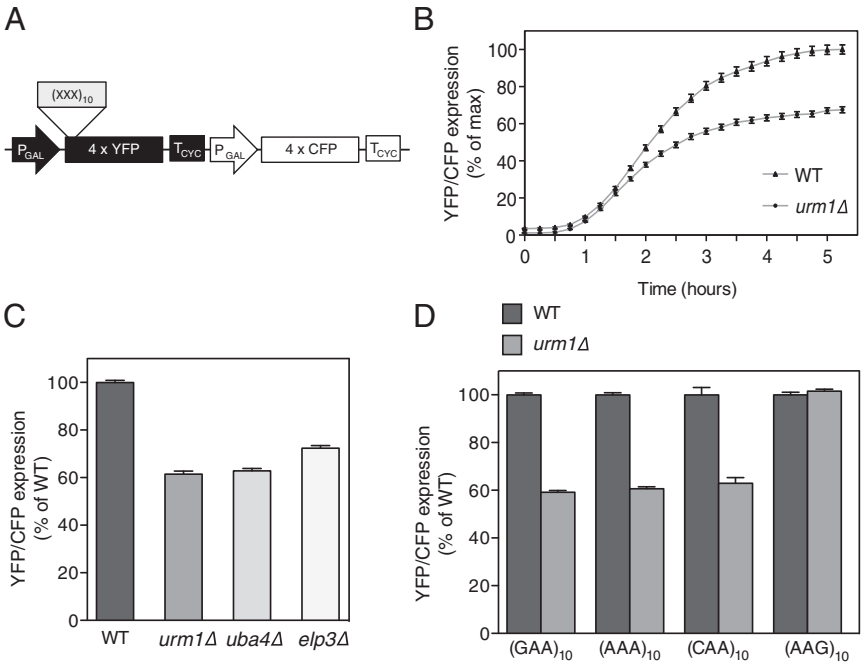

Fig. 4. *URM1* is required for efficient translation of AAA-, GAA-, and CAA-enriched reporters. (*A*) Schematic representation of the dual-fluorescent codon-specific translation reporter. β-Estradiol–inducible quadruple-venus (4× YFP) or quadruple-CFP (4× CFP) proteins serve as codon-specific translation reporters and internal translation control, respectively. Codon-traps composed of a run of 10 identical codons, $(XXX)_{10}$, are inserted at the N-terminus of YFP. (*B*) Time course of $(CAA)_{10}$ translation reporter expression induced at time 0 in wild-type and *urm1*Δ cells. Data show the mean YFP/CFP ratio ± SEM from at least 100 cells plotted as percentage of maximum expression. (*C* and *D*) Expression of the translation reporter after 3-h induction with (*C*) $(CAA)_{10}$ codon-trap in different mutants or (*D*) different codon-traps in wild-type and *urm1*Δ cells. Data show the mean YFP/CFP ratio ± SEM from at least 1,000 cells plotted as percent of wild-type control. See also Fig. S5.

defect in the translation of an AAG codon trap in *urm1*Δ cells, suggesting that thiolated tK^{UUU} only plays a marginal role in the recognition of highly AAG-biased genes. Similarly, although AAA, CAA, and GAA constitute 11.4% of the coding genome, our results indicate that overall translation is not differentially affected in exponentially growing cells lacking a functional *URM1* pathway. Only mRNAs strongly biased in Urm1-dependent codons, such as *CMS1* and *YPL199C*, both of which belong to the upper quartile for AAA and CAA codon abundance, respectively, were translated 50% less efficiently in *urm1*Δ cells. Importantly, we established that the same set of mRNAs was also differentially translated in an *elp3*Δ mutant. These findings are consistent with the dynamic regulation of translation in vivo, where initiation constitutes the rate-limiting step under nonlimiting conditions, but elongation is very fast (31, 32). Interestingly, despite the fact that GAA is more abundant than AAA, our data suggest that the latter is the major cause of differential translation. However, some AAA-, CAA-, and GAA-rich mRNAs did not show the predicted decrease in protein expression levels, suggesting that the position of thiolation-dependent codons in the mRNA may also be important or that compensatory mechanisms may operate in these cases.

Although mutations in the *URM1* and *ELP* pathways increase sensitivity to a number of stresses (12, 33), we found that under rich conditions changes in protein-expression levels are small, and indeed they do not induce a discernable phenotype other than slow growth. Nevertheless, under certain stress conditions small differences in the translation of specific proteins might become relevant. For example, cells lacking components of the *URM1*/*ELP* pathway as well as cells lacking *CMS1*, the translation of which is significantly reduced in *urm1*Δ cells, are associated with quinine sensitivity (34).

Finally, because the proportion of U_{34} modified tRNAs is tissue-dependent and altered by stress (17, 35), both the frequency of *URM1*/*ELP*-dependent codons and the regulation of tRNA posttranscriptional modification might contribute to the fine-tuning of protein expression.

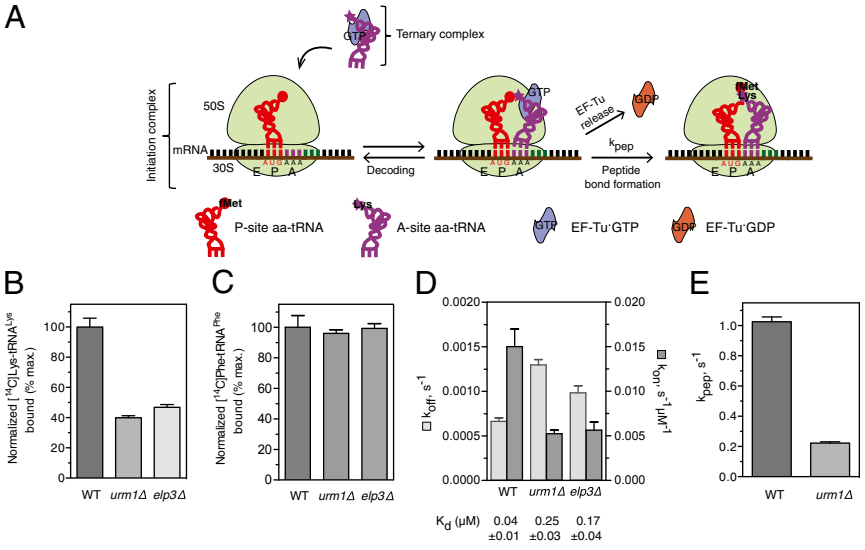

Fig. 5. tRNA thiolation of U_{34} promotes A-site binding and dipeptide formation in vitro. (*A*) Schematic illustration of the decoding and peptide bond formation processes. (*B* and *C*) A-site binding of [^{14}C]Lys-$tRNA^{Lys}$ (*B*) or for control [^{14}C]Phe-$tRNA^{Phe}$ (*C*) isolated from wild-type, *urm1*Δ, or *elp3*Δ cells containing tK^{UUU} ($mcm^5s^2U_{34}$, mcm^5U_{34}, or s^2U_{34} modifications) and tF^{GAA}, were measured after incubation of initiation complex with ternary complex. Data show the mean [^{14}C] signal ± SEM of three independent experiments plotted as percentage of wild-type. (*D*) The rate constants of tRNA dissociation (k_{off}) and tRNA association (k_{on}) of peptidyl-$tRNA^{Lys}$ prepared from wild-type, *urm1*Δ, or *elp3*Δ cells. The equilibrium dissociation constant (K_d) ± SEM is shown below the graph. (*E*) The rate of dipeptide formation (k_{pep}) using $tRNA^{Lys}$ isolated from wild-type and *urm1*Δ cells.

Materials and Methods

Further details on protocols are described in *SI Materials and Methods*.

SILAC Experiments. Cells were labeled with SILAC as described previously (36), and processed and analyzed as described in Fig. S1C.

Quantitative RT-PCR. Quantitative RT-PCR was performed using the SYBR Green I kit (Roche).

[^{35}S] Metabolic Labeling and Polysome Profiles. Equal amounts of cells were pulsed for 15 min with [^{35}S]Met and [^{35}S]Cys (Hartmann Analytics; SCIS-103) and chased for 5 min with cold amino acids. Protein extracts for polysome analysis were separated on a 6–45% sucrose gradient, and ribosome content recorded with a teledyne ISCO UA-6 detector.

Expression of Fluorescent Reporter and Cell Imaging. Expression of the translation reporters was induced with 50 nM β-estradiol and images were taken with an inverted epi-fluorescence microscope (Ti-Eclipse, Nikon). YFP/CFP fluorescence was measured in single cells, and analyzed with YeastQuant software (24).

Cycloheximide Chase. Samples of equal volume were taken at different times after translation block with 100 μg/mL cycloheximide and cell extracts probed with PAP (Sigma; P1291), anti-Pgk1 (Invitrogen; 459250), anti-Act1.

Biochemical and Kinetic Assays. In vitro experiments with purified ribosomes and EF-Tu·GTP·[^{14}C]Lys-tRNA^{Lys} or EF-Tu·GTP·[^{14}C]Phe-tRNA^{Phe} ternary complexes were performed in buffer A (50 mM Tris·HCl pH 7.5, 70 mM NH_4Cl, 30 mM KCl, 7 mM $MgCl_2$). Ribosome complex preparation and experiments testing stability of peptidyl-tRNA binding to the A site were performed as in (37). Quench-flow assays were performed at 24 °C in a KinTek RQF-3 apparatus with 2 μM initiation complex and 0.6 μM ternary complex. Dipeptides were analyzed by RP-HPLC (38).

ACKNOWLEDGMENTS. We thank S. Pelet, S. Leidel, and M. Stark for reagents and advice; members of the M.P. laboratory for discussions; A. Smith and R. Dechant for critical reading of the manuscript; the University of Washington and J. Eng for granting us access to UW SEQUEST v2012.01.2; and David A. Tirrell (California Institute of Technology) for providing the plasmid pQE32-FRS-sc encoding for the His6-tagged phenylalanyl-tRNA synthetase from *Saccharomyces cerevisiae*. V.A.N.R. is a member of the Molecular Life Science doctorate program, and M.P. of the Competence Center for Systems Physiology and Metabolic Diseases. This work is funded in part by the Scottish Institute for Cell Signalling (P.G.A.P.); the College of Life Sciences, University of Dundee, Innovation Pipeline for Translational Science LUPS/ERDF/2008/2/1/0429 (to P.G.A.P.); an Ambizione grant of the Swiss National Science Foundation (to P.G.A.P.); the Scottish Institute for Cell Signalling (K.T.); the College of Life Sciences Bursary at the University of Dundee and by the Discovery Scholarship (to K.T.); the Max Planck Society (M.V.R., A.L.K. and J.M.); and the Deutsche Forschungsgemeinschaft (M.V.R.). This project was supported by the Promedica Foundation, and work in the M.P. laboratory by the European Research Council, the Swiss National Science Foundation, and the Eidgenössische Technische Hochschule Zurich.

1. Czerwoniec A, et al. (2009) MODOMICS: A database of RNA modification pathways. 2008 update. *Nucleic Acids Res* 37(Database issue):D118–D121.
2. Limbach PA, Crain PF, McCloskey JA (1994) Summary: The modified nucleosides of RNA. *Nucleic Acids Res* 22(12):2183–2196.
3. Agris PF, Vendeix FA, Graham WD (2007) tRNA's wobble decoding of the genome: 40 years of modification. *J Mol Biol* 366(1):1–13.
4. Krüger MK, Pedersen S, Hagervall TG, Sørensen MA (1998) The modification of the wobble base of tRNAGlu modulates the translation rate of glutamic acid codons in vivo. *J Mol Biol* 284(3):621–631.
5. Murphy FV, 4th, Ramakrishnan V, Malkiewicz A, Agris PF (2004) The role of modifications in codon discrimination by tRNA(Lys)UUU. *Nat Struct Mol Biol* 11(12): 1186–1191.
6. Takai K, Yokoyama S (2003) Roles of 5-substituents of tRNA wobble uridines in the recognition of purine-ending codons. *Nucleic Acids Res* 31(22):6383–6391.
7. Yarian C, et al. (2002) Accurate translation of the genetic code depends on tRNA modified nucleosides. *J Biol Chem* 277(19):16391–16395.
8. Phelps SS, Malkiewicz A, Agris PF, Joseph S (2004) Modified nucleotides in tRNA(Lys) and tRNA(Val) are important for translocation. *J Mol Biol* 338(3):439–444.
9. Beuning PJ, Musier-Forsyth K (1999) Transfer RNA recognition by aminoacyl-tRNA synthetases. *Biopolymers* 52(1):1–28.
10. Novoa EM, Pavon-Eternod M, Pan T, Ribas de Pouplana L (2012) A role for tRNA modifications in genome structure and codon usage. *Cell* 149(1):202–213.
11. Huang B, Lu J, Byström AS (2008) A genome-wide screen identifies genes required for formation of the wobble nucleoside 5-methoxycarbonylmethyl-2-thiouridine in *Saccharomyces cerevisiae*. *RNA* 14(10):2183–2194.
12. Leidel S, et al. (2009) Ubiquitin-related modifier Urm1 acts as a sulphur carrier in thiolation of eukaryotic transfer RNA. *Nature* 458(7235):228–232.
13. Nakai Y, Nakai M, Hayashi H (2008) Thio-modification of yeast cytosolic tRNA requires a ubiquitin-related system that resembles bacterial sulfur transfer systems. *J Biol Chem* 283(41):27469–27476.
14. Noma A, Sakaguchi Y, Suzuki T (2009) Mechanistic characterization of the sulfur-relay system for eukaryotic 2-thiouridine biogenesis at tRNA wobble positions. *Nucleic Acids Res* 37(4):1335–1352.
15. Schlieker CD, Van der Veen AG, Damon JR, Spooner E, Ploegh HL (2008) A functional proteomics approach links the ubiquitin-related modifier Urm1 to a tRNA modification pathway. *Proc Natl Acad Sci USA* 105(47):18255–18260.
16. Huang B, Johansson MJO, Byström AS (2005) An early step in wobble uridine tRNA modification requires the Elongator complex. *RNA* 11(4):424–436.
17. Chen C, Tuck S, Byström AS (2009) Defects in tRNA modification associated with neurological and developmental dysfunctions in *Caenorhabditis elegans* elongator mutants. *PLoS Genet* 5(7):e1000561.
18. Dewez M, et al. (2008) The conserved Wobble uridine tRNA thiolase Ctu1-Ctu2 is required to maintain genome integrity. *Proc Natl Acad Sci USA* 105(14):5459–5464.
19. Anderson SL, et al. (2001) Familial dysautonomia is caused by mutations of the IKAP gene. *Am J Hum Genet* 68(3):753–758.
20. Umeda N, et al. (2005) Mitochondria-specific RNA-modifying enzymes responsible for the biosynthesis of the wobble base in mitochondrial tRNAs. Implications for the molecular pathogenesis of human mitochondrial diseases. *J Biol Chem* 280(2): 1613–1624.
21. Ting L, et al. (2009) Normalization and statistical analysis of quantitative proteomics data generated by metabolic labeling. *Mol Cell Proteomics* 8(10):2227–2242.
22. Shteynberg D, et al. (2011) iProphet: Multi-level integrative analysis of shotgun proteomic data improves peptide and protein identification rates and error estimates. *Mol Cell Proteomics* 10(12): M111.007690.
23. Louvion JF, Havaux-Copf B, Picard D (1993) Fusion of GAL4-VP16 to a steroid-binding domain provides a tool for gratuitous induction of galactose-responsive genes in yeast. *Gene* 131(1):129–134.
24. Pelet S, Dechant R, Lee SS, van Drogen F, Peter M (2012) An integrated image analysis platform to quantify signal transduction in single cells. *Integr Biol (Camb)* 4(10): 1274–1282.
25. Patil A, et al. (2012) Translational infidelity-induced protein stress results from a deficiency in Trm9-catalyzed tRNA modifications. *RNA Biol* 9(7):990–1001.
26. Björk GR, Huang B, Persson OP, Byström AS (2007) A conserved modified wobble nucleoside (mcm5s2U) in lysyl-tRNA is required for viability in yeast. *RNA* 13(8): 1245–1255.
27. Yarian C, et al. (2000) Modified nucleoside dependent Watson-Crick and wobble codon binding by tRNALysUUU species. *Biochemistry* 39(44):13390–13395.
28. Vendeix FA, et al. (2012) Human tRNA(Lys3)(UUU) is pre-structured by natural modifications for cognate and wobble codon binding through keto-enol tautomerism. *J Mol Biol* 416(4):467–485.
29. Sen GC, Ghosh HP (1976) Role of modified nucleosides in tRNA: Effect of modification of the 2-thiouridine derivative located at the 5′-end of the anticodon of yeast transfer RNA Lys2. *Nucleic Acids Res* 3(3):523–535.
30. Johansson MJO, Esberg A, Huang B, Björk GR, Byström AS (2008) Eukaryotic wobble uridine modifications promote a functionally redundant decoding system. *Mol Cell Biol* 28(10):3301–3312.
31. Kudla G, Murray AW, Tollervey D, Plotkin JB (2009) Coding-sequence determinants of gene expression in *Escherichia coli*. *Science* 324(5924):255–258.
32. Milon P, Konevega AL, Gualerzi CO, Rodnina MV (2008) Kinetic checkpoint at a late step in translation initiation. *Mol Cell* 30(6):712–720.
33. Bauer F, et al. (2012) Translational control of cell division by Elongator. *Cell Rep* 1(5): 424–433.
34. Dos Santos SC, Sá-Correia I (2011) A genome-wide screen identifies yeast genes required for protection against or enhanced cytotoxicity of the antimalarial drug quinine. *Mol Genet Genomics* 286(5–6):333–346.
35. Chan CT, et al. (2010) A quantitative systems approach reveals dynamic control of tRNA modifications during cellular stress. *PLoS Genet* 6(12):e1001247.
36. de Godoy LMF, et al. (2008) Comprehensive mass-spectrometry-based proteome quantification of haploid versus diploid yeast. *Nature* 455(7217):1251–1254.
37. Konevega AL, et al. (2004) Purine bases at position 37 of tRNA stabilize codon-anticodon interaction in the ribosomal A site by stacking and Mg^{2+}-dependent interactions. *RNA* 10(1):90–101.
38. Katunin VI, Muth GW, Strobel SA, Wintermeyer W, Rodnina MV (2002) Important contribution to catalysis of peptide bond formation by a single ionizing group within the ribosome. *Mol Cell* 10(2):339–346.